Biochemical Pharmacology, Vol. 59, pp. 329–336, 2000.

ISSN 0006-2952/00/$–see front matter
PII S0006-2952(99)00332-9

Isolation of a Non-covalent Aldose Reductase–Nucleotide–Inhibitor Complex

*Katsumi Sugiyama, Zhou Chen, Yong S. Lee and Peter F. Kador**

Laboratory of Ocular Therapeutics, National Eye Institute, National Institutes of Health, Bethesda, MD 20892-1850, U.S.A.

ABSTRACT. A method for the isolation of an intact, non-covalent complex formed by the interaction of aldose reductase, NADP(H) nucleotide, and inhibitor has been developed to aid in the discovery and development of novel aldose reductase inhibitors. In the complexes isolated, both the carboxylic acid-containing inhibitor tolrestat and the spirohydantoin-containing inhibitor AL1576 (2,7-difluorospirofluorene-9,5′-imidazolidine-2′,4′-dione) tightly bound in a 1:1 ratio to aldose reductase complexed with either NADPH or $NADP^+$. Inhibitor binding to either the enzyme–$NADP^+$ or enzyme–NADPH complex appeared to be equal and pH-dependent, with maximum binding observed at a pH range of 7 to 8.5 where the inhibitors are ionized. These results indicated that the charge state of the cofactor (NADPH vs $NADP^+$) is not critical for inhibitor binding to aldose reductase. Molecular modeling studies suggested that His110 plays a crucial role in directing charged inhibitors containing either a carboxylate or an ionizable hydantoin group to the active site of aldose reductase by providing charge interaction. BIOCHEM PHARMACOL **59**;4:329–336, 2000. © 2000 Elsevier Science Inc.

KEY WORDS. aldose reductase; diabetes; aldose reductase inhibitors; mechanism of action; non-covalent binding

Excess sorbitol accumulation catalyzed by aldose reductase (EC 1.1.1.21) has been linked to a number of ocular diabetic complications including keratopathy, cataract, and retinopathy [1, 2]. Administration of aldose reductase inhibitors at the onset of diabetes or galactosemia has been shown to prevent corneal epithelial and endothelial changes, osmotic cataract formation, and the selective destruction of retinal capillary pericytes and subsequent formation of microaneurysms and acellular vessels associated with diabetic retinopathy [2, 3]. While a number of structurally diverse compounds inhibit aldose reductase significantly, many of these compounds possess poor pharmacokinetic properties or side-effects not associated with the specific inhibition of aldose reductase [4]. These side-effects range from hydantoin-related skin rash to induction of liver transaminases [5]. These problems reflect a need for the development of new, more potent inhibitors devoid of side-effects.

The design of more potent and specific aldose reductase inhibitors requires an understanding of the interaction between aldose reductase bound to its nucleotide cofactor and its inhibitors and their mechanism of action. Insight into this has come from analyses of a series of crystallized human and porcine aldose reductase–$NADP^+$–inhibitor complexes and molecular modeling studies [6–14]. In addition, specific non-covalent interactions between porcine aldose reductase complexed with $NADP^+$ and inhibitors have been investigated by electrospray mass spectroscopy [15–17]. Here, we report a method for the *in vitro* isolation of a non-covalent complex formed in solution by the interaction of human muscle or rat lens aldose reductase with either $NADP^+$ or NADPH and the aldose reductase inhibitors tolrestat, AL1576, or ponalrestat.

MATERIALS AND METHODS

Unless otherwise stated, all chemicals were of reagent grade, and HPLC solvents were of HPLC grade. NADP(H) was obtained from the Sigma Chemical Co. Microcon™ 10 filter units were obtained from Amicon, Inc. HMAR† was purchased from Wako BioProducts. RLAR expressed in *Escherichia coli* was purified as previously described [18]. The aldose reductase inhibitors AL1576 (2,7-difluorospirofluorene-9,5′-imidazolidine-2′,4′-dione), sorbinil (*S*-6-fluorospirochroman-4,5′-imidazolidine-2′,4′-dione), tolrestat {*N*-[(5-trifluoromethyl-6-methoxy-1-naphthalenyl)thioxomethyl]-*N*-methylglycine}, and ponalrestat {3-([4-bromo-2-fluorobenzyl]-4-oxo-3*H*-phthalazin-1-yl)acetic acid} were gifts from Alcon Laboratories, Pfizer Central Research, Wyeth-Ayerst Research, and ICI Americas, respectively.

* Corresponding author: Peter F. Kador, Ph.D., Building 10, Room 10B-11, National Eye Institute, National Institutes of Health, 10 Center Dr., MSC 1850, Bethesda, MD 20892. Tel. (301) 496-6993; FAX (301) 402-2399.

† *Abbreviations*: HMAR, recombinant human muscle aldose reductase; RLAR, recombinant rat lens aldose reductase; TFA, trifluoroacetic acid; and CHARMM, Chemistry at Harvard Macromolecular Mechanics.

Received 26 March 1999; accepted 9 July 1999.

Determination of Reductase Activity

Aldose reductase activity was determined spectrophotometrically using a Shimadzu spectrophotometer by following the decrease in absorption of NADPH at 340 nm at 25° with dl-glyceraldehyde as substrate [19]. Each 1-mL reaction mixture contained 3 mM NADPH, 1 mM dl-glyceraldehyde, and 0.1 M phosphate buffer at pH 6.2. Reactions were initiated by the addition of enzyme.

Isolation of the Enzyme–Nucleotide–Inhibitor Complex

RLAR and HMAR were purified as previously described, and the nucleotide cofactor was removed by chromatofocusing using a Mono P anion exchange column [18]. The purified enzyme (10 μL of RLAR: 78 pmol; 7 μL of HMAR: 126 pmol) was added to 200 μL of 6.3 mM K/Na phosphate buffer, pH 7.5, containing 6.3% glycerol, 0.63 mM dithiothreitol, and either NADPH or $NADP^+$ (0.03 mM), followed by 5 μL of aldose reductase inhibitors (250 pmol) dissolved in water. The mixture was transferred to the sample reservoir of the Microcon™ 10 filter unit and centrifuged at 16,000 *g* for 15 min to remove excess nucleotide and aldose reductase inhibitor. Each complex was further washed three times with 200 μL of the above phosphate buffer, and the aldose reductase–NADP(H)–inhibitor complex was recovered by placing a sample reservoir upside down in a new vial, adding 40 μL of the same phosphate buffer without cofactor, and centrifuging the sample for 5 min at 16,000 *g*. Binding, indicated by inhibition of reductase activity, was determined by comparing the relative reductase activity in the inhibitor-treated samples with reductase activities in similarly treated control enzyme samples incubated without inhibitor.

Stoichiometric Comparison of Enzyme Activity Loss Versus Amounts of Inhibitor Bound to the Aldose Reductase–Nucleotide–Aldose Reductase Inhibitor Complex

Purified RLAR (78 pmol) was mixed with 250 pmol of either AL1576 or tolrestat; purified HMAR (183 pmol) was mixed with 300 pmol of either AL1576 or tolrestat as described above. Following determination of the remaining reductase activity in aliquots of the purified aldose reductase–nucleotide–inhibitor complexes, the complex was denatured by the addition of methanol to the reservoir of the Microcon™ 10 filter units. The bound aldose reductase inhibitors released from the denatured aldose reductase–nucleotide–inhibitor complexes were collected by centrifugation. The methanol filtrates were dried, dissolved in 100 μL of H_2O, and applied to Sep-Pak C_{18} columns (Millipore Corp.). Following washing of the columns with 3 mL of H_2O to remove K/Na_2 phosphate, glycerol, dithiothreitol, and NADP(H), the retained aldose reductase inhibitors were eluted from the Sep-Pak C_{18} columns with methanol.

The methanolic extracts containing aldose reductase inhibitors were dried, and the residue was analyzed by HPLC using the Pharmacia Smart System (Pharmacia Biotech) equipped with a μRPC C2/C18 PC SC 2.1/10 column operating at room temperature at a flow rate of 0.2 mL/min. The column was equilibrated with H_2O containing 0.05% TFA. After 3 min of equilibration, a linear solvent gradient of 0–60% CH_3CN containing 0.05% TFA was introduced over 10 min followed by a gradient of 60–100% CH_3CN containing 0.05% TFA over the next 3 min. Then the column was re-equilibrated with H_2O containing 0.05% TFA. The eluent was monitored at 254 nm. The amounts of tolrestat and AL1576 bound to RLAR were determined by comparing integrated areas to a corresponding calibration curve. The amounts of tolrestat and AL1576 bound to HMAR were determined using 100 pmol of either inhibitor as an internal standard.

Pseudo-equilibrium and Binding Constants

Using the above binding assay, the pseudo-equilibrium constants of tolrestat and AL1576 (0–400 pmol) with RLAR (78 pmol) and HMAR (123 pmol) were determined using the Briggs–Halden steady-state equation as follows [20]:

$$E + I \underset{k_{-1}}{\overset{k_1}{\rightleftharpoons}} EI \xrightarrow{k_p} EI_b$$

$$\frac{v}{[I]} = -\frac{1}{K_m} v + \frac{V_{max}}{K_m} \qquad K_m = \frac{k_{-1} + k_p}{k_1}$$

The binding equation was modified by substituting $[EI_b]$ or $[I]_b$ for v and $n[E]_t$ for V_{max} where $[I]_b = [EI_b]$ = the concentration of bound inhibitor ∝ % of aldose reductase inhibition, $[E]_t$ = the total enzyme concentration, n = the number of identical and independent inhibitor binding sites per molecule of enzyme, and $n[E]_t$ = the total concentration of inhibitor binding sites. The calculated K_m represents the pseudo-equilibrium or dynamic constant. The reciprocal form of the equation becomes:

$$\frac{n[E]_t}{[I]_b} = \frac{K_m}{[I]} + 1$$

Assuming that one molecule of inhibitor is sufficient to inactivate one molecule of enzyme, then $[I]_b = [E]_t \times$ (% of inhibition of enzyme) and the equation becomes:

$$\frac{100}{\%\text{ of inhibition of enzyme}} = \frac{K_m}{n}\frac{1}{[I]} + \frac{1}{n}$$

By graphing the double-reciprocal plot of 100/% of inhibition of enzyme versus 1/[I], K_m values were obtained from the intercepts of the 100/% inhibition of enzyme and 1/[I] at 1/n and $-1/K_m$, respectively.

pH-Dependence of Enzyme-Nucleotide–Inhibitor Complex Formation

The pH-dependence of the formation of the enzyme–nucleotide–inhibitor complex was investigated using a buffer composed of 2-(*N*-morpholino)ethane-sulfonic acid (0.05 M), Tris (0.1 M), and acetic acid (0.05 M) in which the pH was adjusted at increments of 0.5 between pH 5.5 and 10.0 by the addition of either 0.1 M HCl or 0.1 M NaOH. RLAR (84 pmol) formed complexes with $NADP^+$ and either AL1576 or tolrestat (250 pmol). The complexes were isolated using the Microcon™ 10 filter units as described above, and the reductase activity remaining in the complexes was determined spectrophotometrically at pH 6.2, the pH optimum for aldose reductase.

CHARMM Energy Minimization of the Enzyme–$NADP^+$–Inhibitor Complex

The coordinates of human aldose reductase complexed with NADP(H) and crystal water (lads) [6] were obtained from the Brookhaven Protein Data Bank. Hydrogens were added to the amino acid residues of human aldose reductase using the HBUILD routine of CHARMM [21]. With the exception of His110, all His residues were treated as neutral, with hydrogen assigned to the Nδ1 of neutral histidine. His110 was treated as positively charged, based on the crystallographic evidence that the carboxylate of zopolrestat is salt-linked to the Nε2 hydrogen of His110 [8, 9]. All Asp and Glu residues were assumed to be negatively charged, whereas Arg and Lys were positively charged. AL1576 and tolrestat were docked manually into the active site of aldose reductase complexed with $NADP^+$ so that the ionized group could form hydrogen bonding interactions with Tyr48 and His110. The fluorene ring of AL1576 was stacked against Trp20; the aromatic portion of tolrestat was positioned between Leu300 and Phe122 as reported in the crystal structure [10]. Charge assignment on $NADP^+$, AL1576, and tolrestat, as well as the hydration of the complex of aldose reductase–$NADP^+$–aldose reductase inhibitor and the subsequent energy minimization of the hydrated complex by CHARMM using an all-atom parameter set [22] were carried out on a cluster of HP-735 workstations according to the procedures published elsewhere [13].

RESULTS

Purified RLAR or HMAR, separated from its nucleotide cofactor by chromatofocusing on a Mono P anion exchange column, was dissolved in phosphate buffer, pH 7.5, containing 6.3% glycerol and 0.63 mM dithiothreitol with either NADPH or $NADP^+$. Addition of the carboxylic acid-containing aldose reductase inhibitors tolrestat or ponalrestat or the hydantoin-containing inhibitor AL1576 dissolved in dilute base resulted in the formation of a non-covalent enzyme–nucleotide–inhibitor complex that could be isolated with Microcon™ 10 filter units. After repeated washings with buffer to remove excess inhibitor, the extent of inhibitor binding was determined by comparing the extent of reductase activity remaining in the complexes formed in the presence of inhibitor and nucleotide with that of similar enzyme samples complexed only with nucleotide. As illustrated in Fig. 1, no difference in complex formation was observed when either NADPH or $NADP^+$ was used as a cofactor with tolrestat, ponalrestat, or AL1576. No enzyme–NADP(H)–inhibitor complex was isolated with the hydantoin aldose reductase inhibitor sorbinil. Since sorbinil has an IC_{50} in the micromolar range, this suggests that an inhibitor complex can be isolated only from inhibitors possessing IC_{50} values $< 10^{-7}$ M. No inhibitor–enzyme complex could be isolated in the absence of NADP(H) cofactor.

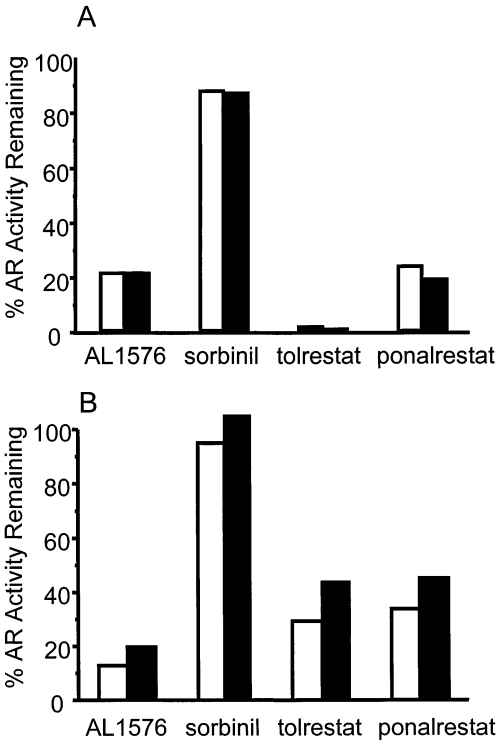

FIG. 1. Comparison of the effect of NADPH (□) or $NADP^+$ (■) on the formation of the enzyme–nucleotide–inhibitor complex in rat lens aldose reductase (A) and human muscle aldose reductase (B) with the aldose reductase inhibitors AL1576, sorbinil, tolrestat, and ponalrestat. The enzyme complex was recovered from Microcon™ 10 filter units after treatment with inhibitors, and the extent of complex formation with inhibitor was expressed as the percent activity remaining, which was determined spectrophotometrically as described in Materials and Methods. N = 2. AR = aldose reductase.

The aldose reductase inhibitors tolrestat and AL1576 bound to the enzyme–NADP(H) complex were recovered by denaturation of the complex with methanol and subsequently quantitated by reverse phase HPLC. Based on the initial amounts of enzyme present, a direct correlation between the loss of enzymatic activity and inhibitor binding was observed (Table 1). This binding appeared to be in a 1:1 ratio.

TABLE 1. Correlation between observed loss of aldose reductase (AR) activity and the amounts of aldose reductase inhibitor (ARI) bound to the AR-NADP(H)-ARI complex as determined by HPLC

Inhibitor	% Activity loss	Inhibitor recovered from complex (pmol)	Ratio [inhibitor]/[enzyme]
RLAR (78 pmol)			
AL 1576	77.4 ± 0.6 (60.2 ± 0.5)*	64.4 ± 7.5	1.05 ± 0.14
Tolrestat	94.5 ± 1.8 (73.5 ± 1.4)	62.7 ± 2.9	0.85 ± 0.05
HMAR (183 pmol)			
AL 1576	78.6 ± 2.0 (143.9 ± 2.0)	155.3 ± 3.7	1.08 ± 0.20
Tolrestat	56.8 ± 1.8 (103.9 ± 1.8)	109.8 ± 2.7	1.06 ± 0.02

Values are means ± SD (N = 3).
* Values in parentheses represent pmol enzyme.

Various amounts of tolrestat and AL1576 also were mixed with fixed amounts of RLAR and HMAR complexed with $NADP^+$. By measuring the reductase activity remaining in the isolated complex and then graphing the data as a double-reciprocal plot of 100/% of inhibition of enzyme versus 1/[I], values for the molar binding ratio (n) and the pseudo-equilibrium constant (K_m) were obtained from the intercepts of 100/% of inhibition of enzyme and 1/[I], respectively (Fig. 2). The n and apparent K_m (nM) values for tolrestat with RLAR were 1.45 ± 0.15 and 85.5 ± 11.2, respectively, and with HMAR they were 1.42 ± 0.16 and 259.2 ± 32.8, respectively. For AL1576, the n and apparent K_m (nM) values with RLAR were 1.00 ± 0.05 and 28.4 ± 1.5, and with HMAR they were 0.99 ± 0.06 and 68.0 ± 9.5.

Whereas the 1:1 molar ratio of AL1576 was in good agreement with the results obtained by denaturing the isolated enzyme–NADP(H)–inhibitor complex determined by HPLC, the kinetically obtained molar binding ratio for tolrestat was considerably higher, i.e. 1.4. Tolrestat in solution is present as *Z*- and *E*-conformers in approximately a 3:1 ratio, and aldose reductase stereoselectively binds only to the *Z*- and not the *E*-conformer of tolrestat as illustrated in Fig. 3. The kinetically determined binding ratio of tolrestat reflects the stereoselective binding of the *Z*-conformer.

As illustrated in Fig. 4, binding of tolrestat and AL1576 to aldose reductase in the isolated non-covalent complex was pH-dependent. The hydantoin AL1576 bound to aldose reductase between pH 7 and 8.5; the carboxylic acid

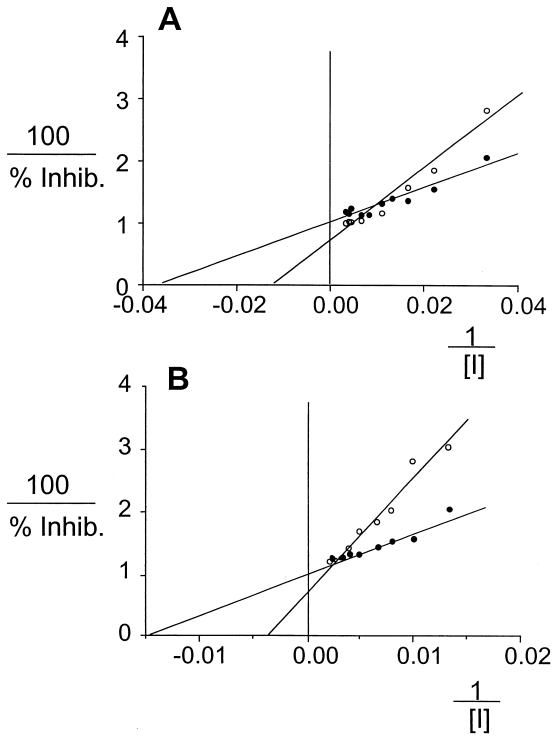

FIG. 2. Double-reciprocal plots for binding of aldose reductase inhibitors AL1576 (●) and tolrestat (○) to aldose reductase complexed with $NADP^+$. Panels A and B represent rat lens aldose reductase and human muscle aldose reductase, respectively.

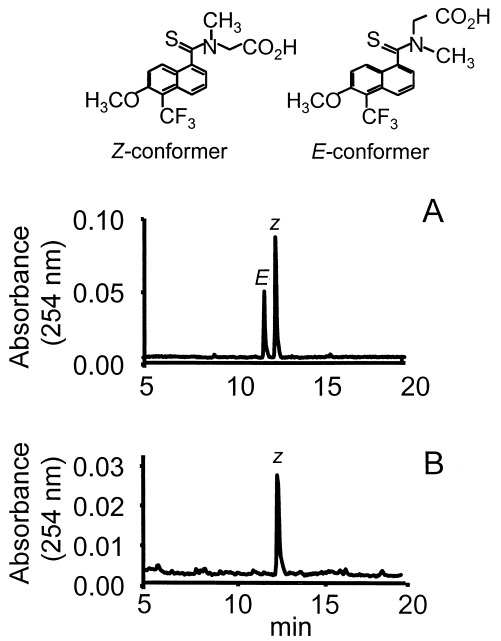

FIG. 3. HPLC elution patterns obtained by C_{18} chromatography of tolrestat, illustrating that only the *Z*-conformer binds with aldose reductase. The elution pattern in A illustrates the presence of both *Z*- and *E*-conformers in the solution of tolrestat used to bind the enzyme–nucleotide complex. The elution pattern in B was obtained by denaturation of the isolated aldose reductase–NADPH–tolrestat complex. See Materials and Methods for details.

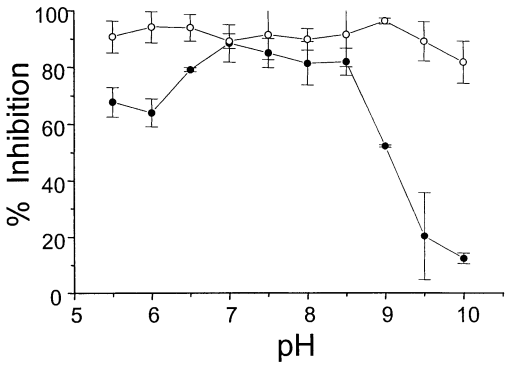

FIG. 4. Effect of pH on the formation of the non-covalent aldose reductase–$NADP^+$–aldose reductase inhibitor complex with the inhibitors AL1576 (●) and tolrestat (○). The enzyme complex was recovered from Microcon™ 10 filter units after treatment with inhibitors, and the extent of complex formation with inhibitor was expressed as the percent inhibition remaining, which was determined spectrophotometrically as described in Materials and Methods. Data are expressed as means ± SD; N = 3.

tolrestat bound to aldose reductase over a broader pH range of 5.5 to 9.

Molecular modeling studies were conducted with tolrestat and AL1576 docked into the substrate binding site of aldose reductase. These studies illustrated that both the hydantoin group of AL1576 and the carboxylate group of tolrestat can form a number of hydrogen bonds with Tyr48, His110, and Trp111 (Figs. 5 and 6). In addition, the 2-fluorine atom of AL1576 and the fluorines on the CF_3 group of tolrestat can hydrogen-bond with the main chain N—H group of Leu300 and the hydroxyl group of Ser302, respectively. These hydrogen bonding interactions are in good agreement with those observed in the crystal structure of porcine ALR2–$NADP^+$–ARI complexes [10]. The energy-minimized structures also indicated that the side chains of Trp20, Trp111, and Phe122 were positioned for van der Waals and aromatic–aromatic interactions with AL1576 and tolrestat.

The distances between the cationic charge center of aldose reductase and the anionic charge center of tolrestat and AL1576 were calculated from the energy-minimized structures (Table 2). The three hetero atoms of the hydantoin ring of AL1576 (Fig. 5) and the two carboxylate oxygen atoms of tolrestat (Fig. 6) were chosen as the anionic charge center; the Nϵ2 hydrogen of His110 and the C4 hydrogen of the nicotinamide group of $NADP^+$ were assigned as the cationic charge center because of their proximity to the anionic center.

DISCUSSION

AL1576, tolrestat, and ponalrestat are tight-binding aldose reductase inhibitors with IC_{50} values in the 10^{-8} M range [18]. They only bind to aldose reductase when the enzyme is complexed with its NADPH or $NADP^+$ cofactor, indicating that these aldose reductase inhibitors bind to the enzyme in an ordered fashion [23]. The present study indicates that these tight-binding inhibitors, when ionized, form a non-covalent enzyme–nucleotide–inhibitor complex that can be isolated using Microcon™ 10 filter units. Based on our inability to isolate a non-covalent enzyme–nucleotide–inhibitor complex with sorbinil, this inhibitor, with

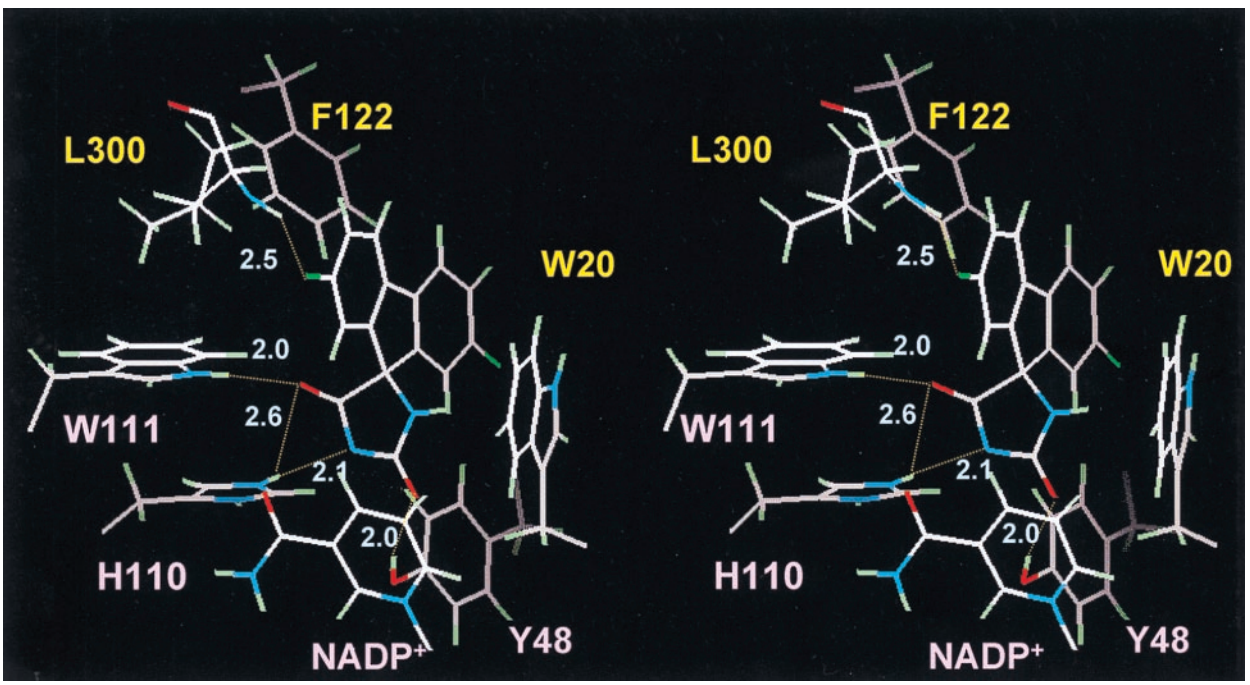

FIG. 5. CHARMM energy-minimized structure of the aldose reductase–$NADP^+$–AL1576 complex. Dotted lines indicate the hydrogen bonding interactions. Atoms represented by colors: white, carbon; green, hydrogen; dark green, fluorine; blue, nitrogen; and red, oxygen.

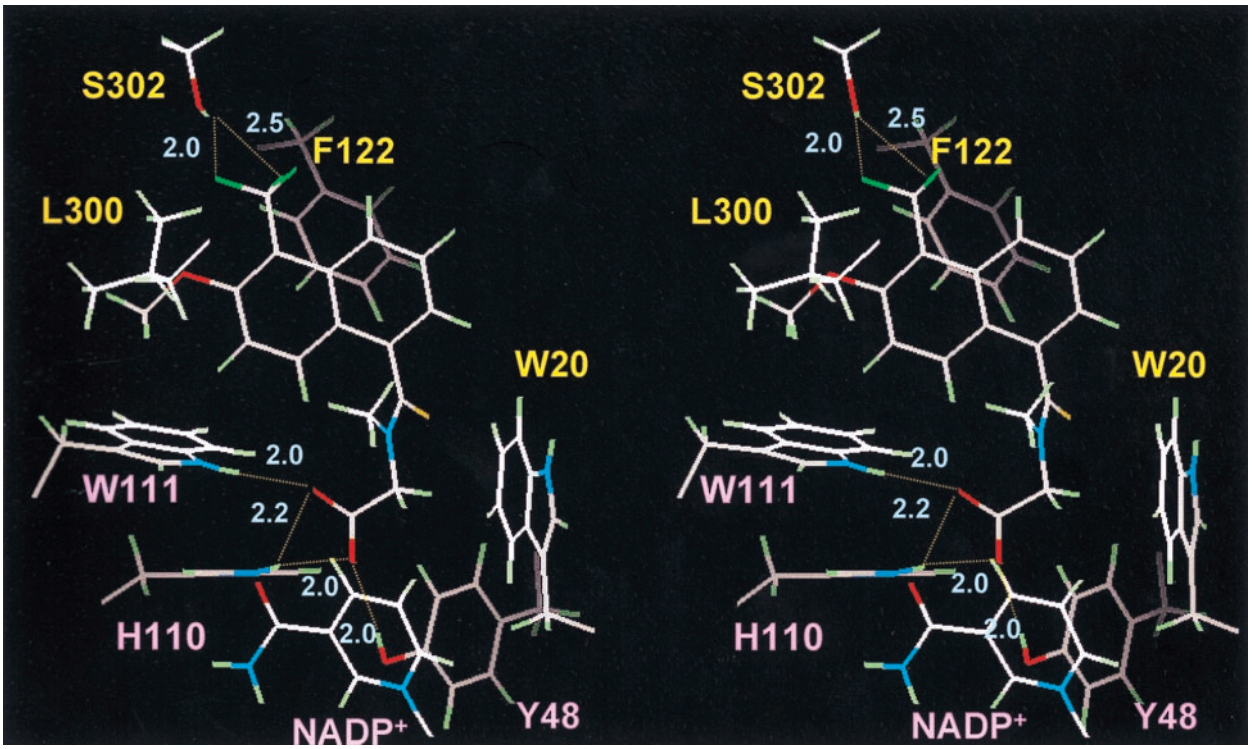

FIG. 6. CHARMM energy-minimized structure of the aldose reductase–NADP$^+$–tolrestat complex. Dotted lines indicate the hydrogen bonding interactions. Atoms represented by colors: white, carbon; green, hydrogen; dark green, fluorine; blue, nitrogen; red, oxygen; and yellow, sulfur.

an IC_{50} of *ca.* 10^{-7} M, does not appear to be tight-binding [18].

pH studies confirmed that the charge complex formed by interaction of the anionic groups of aldose reductase inhibitors and a cationic center within aldose reductase was critical for the formation of the non-covalent enzyme–NADP(H)–inhibitor complex. As illustrated in Fig. 4, as the pH of the buffer increases from 5.5 to 7, the hydantoin group of AL1576 presumably becomes more ionized so that its charge interaction with the cationic center of the enzyme increases. When the pH of the buffer is further increased to 9, this charge interaction decreases due to a loss of the cationic center of the enzyme. A similar pH-dependent loss of a charge interaction at the higher pH also was observed for tolrestat with human aldose reductase (data not shown); however, significant binding of tolrestat with rat lens aldose reductase was still observed under these basic conditions. This may be due to differences in van der Waals interactions and aromatic–aromatic interactions by the aromatic residues at the active site of rat lens aldose reductase compared with human muscle aldose reductase. Contributions from van der Waals interactions and aromatic–aromatic interactions in the formation of the binding complex are evident for AL1576 from the plateaus between pH 7 and 9 and for tolrestat from the plateaus between pH 7 and 9.5. More pronounced pH-dependent charge interactions with no plateau have been observed with inhibitors such as mandelic acid and sorbinil that are not tight-binding [24, 25].

TABLE 2. Distance (Å) between the cationic charge center of aldose reductase (AR) and the anionic charge center of ARIs

	Anionic charge center of inhibitor AL1576			Tolrestat	
Cationic charge center of AR	C2═O	N3	C4═O	O1	O2
Nε2 hydrogen of His110	2.1	2.6	3.7	2.2	2.0
C4 hydrogen of a nicotinamide amide group of NADP$^+$	3.7	4.9	3.5	4.0	3.3

C2═O, C4═O, and N3 are the 2′ and 4′ oxygen and 3′ nitrogen of the hydantoin group of Al1576 (Fig. 5), and O1 and O2 represent the oxygen atoms of the carboxylate of tolrestat (Fig. 6).

The source of the "cation sink" in the substrate binding site of aldose reductase is controversial. From crystallographic and kinetic studies [24, 26], it has been concluded that the primary source is NADP$^+$ and that aldose reductase inhibitors bind preferentially with the enzyme–NADP$^+$ complex. However, with fluorometric methods it has been reported that the aldose reductase inhibitor sorbinil preferentially interacts with the enzyme–NADPH complex, whereas zopolrestat binds equally well to aldose reductase complexed with either NADPH or NADP$^+$ [27]. The present results indicate that there is no difference in inhibitor binding to form the non-covalent enzyme–inhibitor complex with either NADPH or NADP$^+$ for any inhibitor examined (Fig. 1). This finding is in contrast to the non-competitive behavior of aldose reductase inhibitors, which suggests that inhibitors preferentially bind to

the enzyme–$NADP^+$ complex. Since the catalytic mechanism of aldose reductase is believed to be an Ordered Bi Bi system, with the release of $NADP^+$ rather than the reduction of substrate being the rate-determining step [23, 27], competition between substrate and inhibitor at the active site is masked in the overall rate of the reaction. As a consequence, the inhibition at the active site upon the release of product gives rise to non-competitive behavior of aldose reductase inhibitors.

The present binding assay indicated that the charge state of the cofactor (NADPH vs $NADP^+$) was not critical for inhibitor binding to aldose reductase. These observations support the previous conclusion obtained through molecular modeling studies [13] that His110 plays a crucial role in directing charged inhibitors containing either a carboxylate or an ionizable hydantoin group to the active site of aldose reductase by providing charge interaction. This conclusion also is supported by the crystallographic finding that His110 of aldose reductase forms a salt-bridge to the carboxylate of the zopolrestat complex [8, 9]. Although it is possible that a water molecule hydrogen bonded to the Nδ1 of His110 provides a proton, the exact mechanism of formation of doubly protonated His110 is not known. As demonstrated in the calculated distances between the anionic charge center of tolrestat and AL1576 and the cationic charge center on either the Nϵ2 hydrogen of His110 or the C4 hydrogen of the nicotinamide group of $NADP^+$ (Table 2), the distance between the anionic charge of the inhibitors and the Nϵ2 hydrogen of His110 is 2.2 to 3.7 Å, compared with 3.3 to 4.9 Å for the distance between the anionic charge of the inhibitors and the C4 hydrogen of the nicotinamide group of $NADP^+$. In addition to a shorter distance to the anionic charge center, the Nϵ2 hydrogen of His110 is oriented to form hydrogen-bonding interactions with the ionized portion of the inhibitors (Figs. 5 and 6). Therefore, the charge interaction between the Nϵ2 hydrogen of His110 and the anionic charge of the inhibitors is favored over the charge interaction with the C4 hydrogen of the nicotinamide group of $NADP^+$. This explains the observed comparable binding affinity of tolrestat and AL1576 with aldose reductase complexed with either NADPH or $NADP^+$.

Both AL1576 and *Z*-tolrestat bind to aldose reductase complexed with NADP(H) in a 1:1 ratio to form a non-covalent complex. Since only the *Z*-rotamer of tolrestat binds with the aldose reductase–nucleotide complex [14] and the ratio of *Z*- and *E*-rotamers of tolrestat in solution is 3 to 1 [28], kinetic studies incorrectly indicate that 1.4 molecules of tolrestat are required to inhibit 1 molecule of aldose reductase.

The present binding method enables one to isolate the non-covalent enzyme–NADP(H)–inhibitor complex formed with potent, tight-binding aldose reductase inhibitors. This method is particularly applicable for the isolation of potent inhibitors obtained from combinatorial chemistry and biological samples. Therefore, this method may be useful for the discovery and development of novel, therapeutic aldose reductase inhibitors for the prevention of diabetic complications.

References

1. Kinoshita JH, Aldose reductase in the diabetic eye. XLIII Edward Jackson Memorial Lecture. *Am J Ophthalmol* **102:** 685–692, 1986.
2. Kador PF, The role of aldose reductase in the development of diabetic complications. *Med Res Rev* **8:** 325–352, 1988.
3. Neuenschwander H, Takahashi Y and Kador PF, Dose-dependent reduction of retinal vessel changes associated with diabetic retinopathy in galactose-fed dogs by the aldose reductase inhibitor M79175. *J Ocul Pharmacol Ther* **13:** 517–528, 1997.
4. Pfeifer MA, Schumer MP and Gelber DA, Aldose reductase inhibitors: The end of an era or the need for different trial designs? *Diabetes* **46**(Suppl 2)**:** 82–89, 1997.
5. Spielberg SP, Shear NH, Cannon M, Hutson NJ and Gunderson K, *In-vitro* assessment of a hypersensitivity syndrome associated with sorbinil. *Ann Intern Med* **114:** 720–724, 1991.
6. Wilson DK, Bohren KM, Gabbay KH and Quiocho FA, An unlikely sugar substrate site in the 1.65 Å structure of the human aldose reductase holoenzyme implicated in diabetic complications. *Science* **257:** 81–84, 1992.
7. Rondeau J-M, Tête-Favier F, Podjarny A, Reymann J-M, Barth P, Biellmann J-F and Moras D, Novel NADPH-binding domain revealed by the crystal structure of aldose reductase. *Nature* **355:** 469–472, 1992.
8. Wilson DK, Tarle I, Petrash JM and Quiocho FA, Refined 1,8 Å structure of human aldose reductase complexed with the potent inhibitor zopolrestat. *Proc Natl Acad Sci USA* **90:** 9847–9851, 1993.
9. Wilson DK, Nakano T, Petrash JM and Quiocho FA, 1.7 Å structure of FR-1, a fibroblast growth factor-induced member of the aldo-keto reductase family, complexed with coenzyme and inhibitor. *Biochemistry* **34:** 14323–14330, 1995.
10. Urzhumtsev A, Tete-Favier F, Mitschler A, Barbanton J, Barth P, Urzhumtseva L, Biellmann J-F, Podjarny A, and Moras D, A 'specificity' pocket inferred from the crystal structures of the complexes of aldose reductase with the pharmaceutically important inhibitors tolrestat and sorbinil. *Structure* **5:** 601–612, 1997.
11. Kador PF and Sharpless N, Aldose reductase inhibitors: A potential new class of agents for the pharmacological control of certain diabetic complications. *J Med Chem* **28:** 841–849, 1985.
12. Lee YS, Pearlstein R and Kador PF, Molecular modeling studies of aldose reductase inhibitors. *J Med Chem* **37:** 787–792, 1994.
13. Lee YS, Chen Z and Kador PF, Molecular modeling studies of the binding modes of aldose reductase inhibitors at the active site of human aldose reductase. *Bioorg Med Chem* **6:** 1811–1819, 1998.
14. Lee YS, Sugiyama K and Kador PF, Rotamers of tolrestat and their binding mode to aldose reductase. *Adv Exp Med Biol* **463**: 465–472, 1999.
15. Jaquinod M, Potier N, Klarskov K, Reyman JM, Sorokine O, Kieffer S, Barth P, Andriantomanga V, Biellmann J-F and Van Dorsselaer A, Sequence of pig lens aldose reductase and electrospray mass spectrometry of non-covalent and covalent complexes. *Eur J Biochem* **218:** 893–903, 1993.
16. Potier N, Barth P, Tritsch D, Biellmann J-F and Van Dorsselaer A, Study of non-covalent enzyme-inhibitor complexes of aldose reductase by electrospray mass spectrometry. *Adv Exp Med Biol* **414:** 453–454, 1997.
17. Potier N, Barth P, Tritsch D, Biellmann J-F and Van

Dorsselaer A, Study of non-covalent enzyme-inhibitor complexes of aldose reductase by electrospray mass spectrometry. *Eur J Biochem* **243:** 274–282, 1997.
18. Sato S, Old S, Carper D and Kador PF, Purification and characterization of recombinant human placental and rat lens aldose reductases expressed in *Escherichia coli*. *Adv Exp Med Biol* **372:** 259–268, 1995.
19. Sato S and Kador PF, Inhibition of aldehyde reductase by aldose reductase inhibitors. *Biochem Pharmacol* **40:** 1033–1042, 1990.
20. Segel IH, *Enzyme Kinetics*, pp, 25–29 and 218–220. Wiley-Interscience Publications, New York, 1975.
21. Brooks BR, Bruccoleri RE, Olafson BD, States DJ, Swaminathan S and Karplus M, A program for macromolecular energy minimizations and molecular dynamics calculations. *J Comput Chem* **4**: 187–217, 1983.
22. Molecular Simulation Inc., Parameter file for CHARMm version 22, Waltham, MA, 1992.
23. Grimshaw CE, Shahbaz M and Putney CG, Mechanistic basis for nonlinear kinetics of aldehyde reduction catalyzed by aldose reductase. *Biochemistry* **29:** 9947–9955, 1990.
24. Grimshaw CE, Bohren KM, Lai C-J and Gabbay KH, Human aldose reductase: p*K* of tyrosine 48 reveals the preferred ionization state for catalysis and inhibition. *Biochemistry* **34:** 14374–14384, 1995.
25. Liu SQ, Bhatnagar A and Srivastava SK, Does sorbinil bind to the substrate binding site of aldose reductase? *Biochem Pharmacol* **44:** 2427–2429, 1992.
26. Ehrigh T, Bohren KM, Prendergast FG and Gabbay KH, Mechanism of aldose reductase inhibition: Binding of $NADP^+$/NADPH and alrestatin-like inhibitors. *Biochemistry* **33:** 7157–7165, 1994.
27. Nakano T and Petrash JM, Kinetic and spectroscopic evidence for active site inhibition of human aldose reductase. *Biochemistry* **35:** 11196–11202, 1996.
28. Lee H-K and Querijero G, Kinetics and mechanisms of thioamide rotational isomerism: *N*-thionaphthoyl-*N*-methyl glycine derivative. *J Pharm Sci* **74:** 273–276, 1985.